Materials Research Proceedings 64 (2026) 615-623 https://doi.org/10.21741/9781644904091-77

Structural and Thermal Performance Analysis of (In,Ga)N p–i–n Homojunction Solar Cells

Hassan ABBOUDI[1,a*], Ilyass EZ-ZEJJARI[2,b*], Haddou EL GHAZI[2,c], Redouane EN-NADIR[3,d], Redouane SERSAR[2,e], Walid BELAID[5,f], Ahmed SALI[1,g]

[1]LPS, Faculty of sciences, Sidi Mohamed Ben Abdellah University, Fez 30000, Morocco

[2]LCCPS, ENSAM, Hassan 2 University, 150 Bd du Nil, Casablanca 20670, Morocco

[3]Interdisciplinary Institute for Technological Innovation, Sherbrooke University, 2500 Bd University, Sherbrooke, Canada

[5]Pollard Institute, School of Electronic and Electrical Engineering, University of Leeds, Leeds, United Kingdom

[a]hassan.abboudi@usmba.ac.ma, [b]ilyass.ezzejjari-etu@etu.univh2c.ma, [c]elghazi.haddou@ensam-casa.ma, [d]radouane.en-nadir@usherbrooke.ca, [e]redouane.sersar-etu@etu.univh2c.ma, [f]w.belaid@leeds.ac.uk, [g]ahmed.sali@usmba.ac.ma

Keywords: p-i-n Photovoltaic Cells, Intrinsic Layer, Temperature, Efficiency

Abstract. This study examines the combined influence of intrinsic layer thickness and temperature on the performance of (In,Ga)N-based p–i–n solar cells using SCAPS-1D simulation. The structure, composed of $p - In_{0.6}Ga_{0.4}N/i - In_xGa_{1-x}N/n - In_{0.48}Ga_{0.52}N$ layers, is analyzed under 300K and 400 K to assess thermal effects on carrier transport and recombination. The optimal performance was obtained for an indium molar fraction of $x = 0.59$. The Results reveal that the thickness engineering significantly enhances current generation up to $\sim 0.5\ \mu m$, beyond which absorption saturation limits further improvement. While V_{oc} and FF remain nearly thickness-independent, both degrade with rising temperature due to thermally activated recombination. Overall, the conversion efficiency benefits from optimal intrinsic layer thickness and controlled operating temperature, highlighting the importance of structural and thermal optimization for high-performance (In,Ga)N-based solar cells.

Introduction.

Solar cells represent a promising solution to the global energy crisis. However, their large-scale adoption is limited by the high cost of fabrication and comparatively modest power conversion efficiencies. In Consequence, enhancing the photovoltaic efficiency of thin-film device architectures remains a major research challenge. Recent advances in the growth of III-nitride semiconductors, particularly InGaN, have opened new opportunities for photovoltaics [1, 2]. This material is caracterised by its thermal stability, radiation tolerance, and high absorption coefficient [3, 4]. Its tunable bandgap (0.70-3.42 eV) allows absorption across a wide solar spectrum, from infrared to ultraviolet. Due to these properties, InGaN is considered a potential material for high-efficiency solar photovoltaic cells, both single and multi-junction [5, 6]. The p–i–n architecture further improve charge separation and transport [7, 8], boosting the performance of nitride-based devices. This configuration optimise carrier collection, reduces optical losses, and increases defect tolerance. Numerical simulations of $In_xGa_{1-x}N$ devices have reported efficiencies ranging from 8.9% to 18.74% through adjustments in indium composition, layer thickness, and doping [9, 10]. Most studies have considered these parameters separately, neglecting their combined impact, despite the critical influence of environmental factors like temperature and humidity on solar cell performance.

Content from this work may be used under the terms of the Creative Commons Attribution 3.0 license. Any further distribution of this work must maintain attribution to the author(s) and the title of the work, journal citation and DOI. Published under license by Materials Research Forum LLC.

The influence of temperature on (In,Ga)N p–i–n structures has not been extensively studied. The first photovoltaic response from an InGaN/GaN double heterostructure with a 0.2 μm active layer was notably reported by Jani et al. [11], who achieved an internal quantum efficiency of 60% and an open-circuit voltage of 2.4 V. Subsequent work by Neufeld et al. [12] demonstrated enhanced performance, reaching a maximum external quantum efficiency of 63% and a current density of 4.2 mA/cm². We conduct a comprehensive numerical study of $Ga_{1-x}In_xN$ p-i-n junction using SCAPS-1D software. Under standard AM1.5D irradiance, the impact of temperature on key photovoltaic metrics including open-circuit voltage, short-circuit current density, fill factor, and efficiency is systematically analyzed. This paper is structured in four main sections. Following this introduction, which establishes the research objectives and methodological foundation, Section 2 develop the theoretical framework and describes the simulation techniques employed. Section 3 present the numerical results and provides a comprehensive discussion of their implications. Finally, Section 4 summarizes the principal conclusions and highlights potential directions for future investigation.

Theoretical Modeling and simulation.

Figures 1 illustrates the architecture of the p-i-n photovoltaic cell analyzed in this study. The device employs a specific layer sequence of $p-In_{0.6}Ga_{0.4}N/i-In_xGa_{1-x}N/n-In_{0.48}Ga_{0.52}N$. The compositional grading of the p- and n-type layers, with indium mole fractions of 0.6 and 0.48 respectively, was implemented based on prior optimization [13]. The p-type layer functions as a hole-transport and buffer layer, while the n-type layer facilitates electron transport and acts as an optical window. At the core of the device, the intrinsic absorber layer $i-In_xGa_{1-x}N$ is designed to maximize photon absorption and carrier generation. The simulations indicate that the optimal photovoltaic performance is achieved for indium (In) content $x = 0.59$. Under operational illumination, the intrinsic region is fully depleted, establishing a significant internal electric field that enhances electron-hole pair separation and collection efficiency by suppressing bulk recombination. Device performance simulations were carried out using the SCAPS-1D, considering the standard AM1.5G solar spectrum.

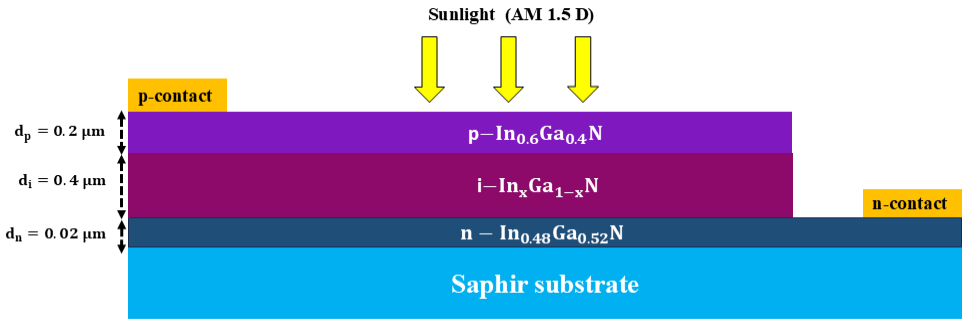

***Fig 1**.Schematic representation of p–i–n (In,Ga)N homojunction solar cell architecture.*

This work investigates the impact of intrinsic layer (i-layer) thickness on the performance of (In,Ga)N based solar cells, evaluating the key photovoltaic parameters; open-circuit voltage V_{oc}, short-circuit current density j_{sc} , fill factor FF, and conversion efficiency η as functions of the i-layer thickness. The analysis also considers thermal effects by examining how these parameters vary with i-layer thickness at two different temperatures: 300 K, and 400 K. Device simulations were carried out using SCAPS-1D, which numerically solves the Poisson equation, electron-hole continuity equations, and the drift-diffusion approach within a one-dimensional framework [14]. By incorporating realistic boundary conditions, material parameters, and recombination mechanisms through Shockley-Read-Hall (SRH) carrier recombination formalism, SCAPS-1D provides a rigorous framework for analyzing carrier dynamics and performance limitations [15].

Materials Research Proceedings 64 (2026) 615-623 https://doi.org/10.21741/9781644904091-77

$$\frac{\partial^2\psi(x)}{\partial x^2} = \frac{e}{\varepsilon_0\varepsilon_r}\left(p(x) - n(x) + N_d - N_a + \rho_p - \rho_n\right) \quad (1)$$

Where; ψ denotes the electrostatic potential, $p(x)$ and $n(x)$ represent the hole and electron concentrations, respectively. ε_0 is the vacuum permittivity, ε_r is the relative permittivity, and e is the elementary charge. N_a and N_d present the acceptor and donor concentrations, respectively, while ρ_n and ρ_p correspond to electrons and holes spatial distributions. Accurate performance modeling of $In_xGa_{1-x}N$ solar cells therefore necessitate precise determination of the alloy's material parameters. Among these, the bandgap energy E_g of $In_xGa_{1-x}N$ is represented as a function of indium content as [16].

$$E_g^{In_xGa_{1-x}N}(x,T) = x \cdot E_g^{InN}(T) - (1-x) \cdot E_g^{GaN}(T) - bx(1-x) \quad (2)$$

b present the band gap bowing parameter, b=1.43 **[17]**.

$E_g^{InN}(T), E_g^{GaN}(T)$ denote the temperature-dependent bandgap energies of GaN and InN, which are commonly expressed using the Varshni formulas [18]:

$$E_g(A,T) = E_g(A,0) - \frac{\alpha T^2}{T+\beta} \quad (3)$$

Where $E_g(A,0)$ is the gap of a given semi-conductor a (GaN, InN) at T= 0 K.

The relative permittivity ε_r and the electron affinity χ are defined as:

$$\varepsilon^*(x,T) = x \cdot \varepsilon^*_{InN}(T) + (1-x) \cdot \varepsilon^*_{GaN}\ (T) \quad (4)$$

$$\chi(In_xGa_{1-x}N) \approx x\chi^{InN}(T) + (1-x)\chi^{GaN}(T) \quad (5)$$

The temperature-dependent effective density of states for the conduction N_c and valence N_v bands is given by:

$$N_c(In_xGa_{1-x}N) = xN_c^{InN}(T) + (1-x)N_c^{GaN}(T) \quad (6)$$

$$N_v(In_xGa_{1-x}N) = xN_v^{InN}(T) + (1-x)N_v^{GaN}(T) \quad (7)$$

Solar cell efficiency depends on three fundamental performance metrics: V_{oc}, J_{sc} and FF. The open circuit voltage V_{oc} and fill factor FF are given by the following expressions **[19]**:

$$V_{oc} = \frac{K_B T}{q} \ln\left(\frac{J_{sc}}{J_o} + 1\right) \quad (8)$$

$$FF = \frac{v_{oc} - \ln(v_{oc} + 0.72)}{v_{oc} + 1} \quad (9)$$

Where $v_{oc} = qV_{oc}/kT$.

Finally, the solar cell efficiency η, defined as the ratio of output power to input power P_{in}, is given by the following expression [20]:

$$\eta = \frac{FF.V_{oc} \cdot J_{sc}}{P_{in}} \quad (10)$$

Where P_{in} represents the optical input power of solar radiation under standard AM1.5G illumination, corresponding to 100 W/cm² at the cell surface.

Materials Research Proceedings 64 (2026) 615-623 https://doi.org/10.21741/9781644904091-77

We summarize in Table 1 all the physical input parameters used in this study.

Table 1. *Room-temperature physical parameters of the materials employed in the simulation.*

Layer	E_g(eV)	χ(eV)	$\varepsilon_r(F.m^{-1})$	$N_c(1.10^{18}cm^{-3})$	$N_v(1.10^{19}cm^{-3})$
$In_{0.6}Ga_{0.4}N$	1.399	5.144	12.98	1.44	4.967
$In_{0.59}Ga_{0.41}N$	1.422	5.127	12.922	1.455	4.96
$In_{0.48}Ga_{0.52}N$	1.705	4.943	12.284	1.6	4.898

Results and discussion.

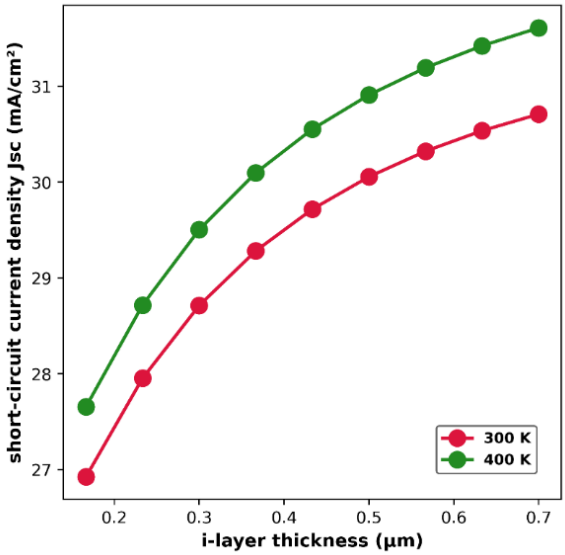

Fig 2. *Dependence of the short-circuit current density j_{sc} on the i-layer thickness at two different temperatures.*

Figure 2 presents the variation of j_{sc} with intrinsic layer thickness over the range of 0.1- 0.7 µm, under two different temperatures 300 K, and 400 K and the optimal photovoltaic performance is achieved for an indium concentration of $x = 0.59$. As a results, j_{sc} increases with intrinsic layer thickness until it progressively saturates beyond a critical thickness of $d_i \approx 0.5$ µm. this behaviour reflects the direct influence of the absorbing region on the generation of photo-induced carriers: a thicker intrinsic layer d_i enhances photon absorption and increases carrier generation, but beyond a certain threshold, most useful photons are already absorbed, making the additional gain marginal. For illustration, j_{sc} rises from 26.8, and 27.6 mA.cm^{-2} at 300 K, and 400 K, respectively, for d_i = 0.16 µm, to about 29.9, and 30.7 mA.cm^{-2} at 0.5 µm, before reaching 30.4, and 31.6 mA.cm^{-2} at 0.7 µm, thus confirming the saturation. The increase in thickness from 0.16 to 0.5 µm therefore corresponds to a relative improvement of 11.57% at 300 K, and 11.23% at 400 K. In parallel, temperature exerts a notable effect: for a thickness of d_i = 0.5 µm, increasing the temperature from 300 K to 400 K provides an additional 0.8 mA.cm^{-2}, leading to an overall improvement of 2.6% between 300 K and 400 K. This trend suggests that higher temperature enhances the collection of photogenerated carriers, likely due to improved mobility and a reduction of the band gap energy. These results therefore demonstrate that the intrinsic layer thickness is a critical parameter for the optimization of $p - In_{0.6}Ga_{0.4}N/i - In_xGa_{1-x}N/n - In_{0.48}Ga_{0.52}N$ solar cells With x = 0.59, this composition is considered throughout the entire study presented in this article. Increasing the thickness significantly improves current generation up to an optimal threshold (0.5 µm), beyond which further gains become negligible due to absorption saturation.

Materials Research Proceedings 64 (2026) 615-623 https://doi.org/10.21741/9781644904091-77

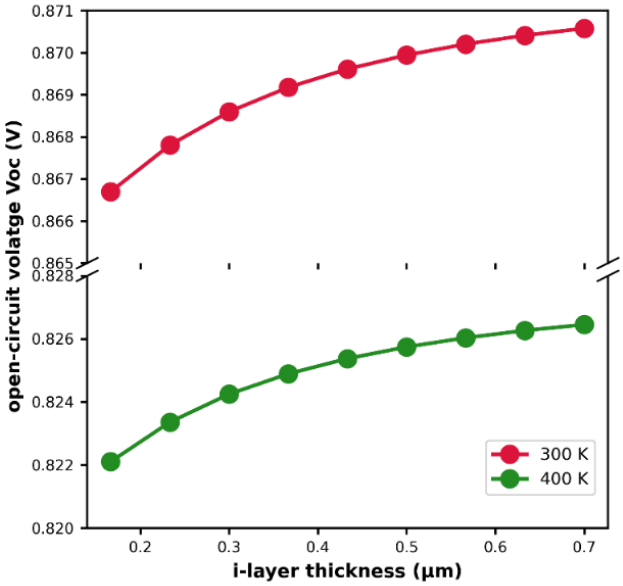

***Fig 3**. Evolution of the open-circuit voltage V_{oc} as a function of the intrinsic layer thickness, analyzed at two distinct temperatures.*

The variation of V_{oc} as a function of i-layer thickness d_i in the range of 0.1-0.7 µm is shown in Figure 3 under two operating temperatures. A consistent trend is observed across all temperatures: V_{oc} exhibits only a very slight increase, such that it can be considered practically constant with respect to d_i. This indicates that, in this configuration, V_{oc} is mainly governed by temperature dependent mechanisms rather than by variations in absorption length or carrier generation efficiency. Indeed, at 300 K, V_{oc} retains a relatively high value of approximately 0.87 V, with a slight increase of about 0.69% across the entire range of intrinsic layer thicknesses. At 400 K, this voltage slightly decreases, varying from 0.823 V to 0.826 V, corresponding to a relative decrease of 5.32% over the same d_i range. Consequently, the variation in V_{oc} remains below 1% within the studied range, indicating a weak sensitivity of this parameter to the intrinsic layer thickness, regardless of temperature. Meanwhile, the significant reduction in V_{oc} observed at higher temperatures aligns with the fundamental principle that the saturation current density j_0 exhibits an exponential dependence on temperature. Indeed, at high temperatures, for example 400 K, carrier excitation and SRH recombination are enhanced, leading to an increase in j_0 and a reduction in V_{oc}. The intrinsic layer thickness mainly affects j_{sc}, while remains largely insensitive to these variations. The strong temperature dependence highlights the importance of minimizing thermally activated recombination and controlling defects to maintain a high V_{oc} under optimal operating conditions.

Materials Research Proceedings 64 (2026) 615-623 https://doi.org/10.21741/9781644904091-77

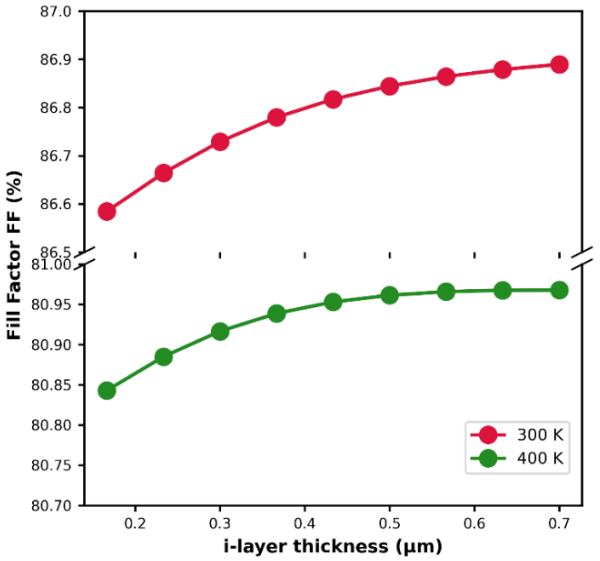

Fig 4. *Variation of the fill factor (FF) as a function of the intrinsic layer thickness, investigated at two distinct temperatures.*

The dependence of FF as a function of i-layer thickness d_i ($0.1 - 0.7$ μm) at 300K and 400K is presented in Figure 4. The results indicate that FF is nearly independent of d_i, exhibiting minimal variation ($< 0.5\%$) across the studied range. In contrast, FF shows a strong temperature dependence: it reaches a maximum of about $86.5 - 86.9\%$ at 300 K, and further declines to 80.85-80.95% at 400 K. As temperatures rise, we observe a decrease in performance. This is largely due to thermally activated recombination and leakage currents, combined with a reduction in carrier mobility. These issues increase the device's internal resistance, making it harder to extract power effectively. The invariance of FF with thickness implies that resistive and recombination mechanisms remain largely unaffected by absorption depth, unlike the short-circuit current density. Hence, optimizing FF in (In,Ga)N based solar cells requires focusing on thermal management, defect passivation, and resistance reduction rather than modifying the intrinsic layer thickness.

Figure 5 depicts the variation of the power conversion efficiency η as a function of the intrinsic layer thickness at two distinct temperatures. The results reveal a general behaviour of increasing efficiency with increasing intrinsic layer thickness, although the absolute values are strongly dependent on the operating temperature. At 300 K, the device exhibits its highest performance, with the efficiency rising from 20.2% to 23.4% over the same range of thickness from $d_i = 0.16$ μm to $d_i = 0.7$ μm, resulting in a relative increase of approximately 15.84%. In contrast, at 400 K, a pronounced degradation is observed: η increases from 18.3% to 20.8%, representing a 13.66% relative improvement, yet with absolute values significantly lower than those obtained at 300 K. A comparative analysis further shows that the sensitivity to temperature becomes more pronounced with thickness. For thin layers $d_i = 0.16$ μm, the efficiency differs by 1.9% between 300 K (20.2%) and 400 K (18.3%), while for thicker layers $d_i = 0.7$ μm, the difference increases to 2.6% between 300 K (23.4%) and 400 K (20.8%). Efficiency increases with intrinsic layer thickness up to 0.5 μm, beyond which recombination limits gains. Temperature strongly affects performance, peaking at 300 K and dropping at 400 K owing to intensified recombination mechanisms and reduced charge carrier mobility. Both factors are thus critical for device efficiency.

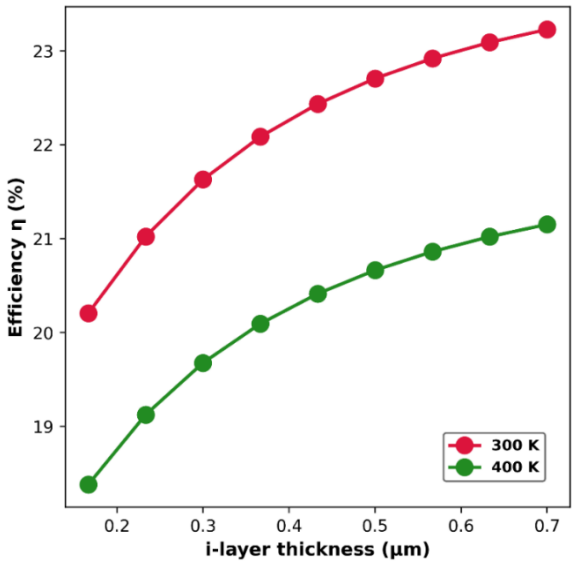

Fig 5. *Efficiency variation with intrinsic layer thickness, investigated across two temperatures.*

Conclusion

The performance of (In,Ga)N p-i-n photovoltaic devices has been systematically analyzed via SCAPS-1D simulations, with a dedicated focus on the interaction between the i-layer thickness and temperature. These findings demonstrate that the intrinsic layer thickness plays a pivotal role in device optimization: increasing d_i enhances current generation up to an optimal value of approximately 0.5 μm, beyond which further improvements are limited by absorption saturation. In contrast, V_{oc} remains largely unaffected by thickness variations but decreases monotonically with increasing temperature, consistent with thermally enhanced recombination mechanisms. Similarly, while the fill factor FF is invariant with respect to thickness, it exhibits a temperature-induced degradation, declining from 86.9% at 300 K to 80.95% at 400 K. In summary, the conversion efficiency benefits from both thickness engineering and thermal management. Efficiency improves with increasing d_i across all temperatures, although the gains diminish beyond the 0.5 μm threshold, whereas temperature exerts a more pronounced influence: the optimal performance is achieved at 300 K, while heating to 400 K induces a $10 - 12\%$ efficiency loss relative to room temperature. These results underscore the crucial importance of carefully balancing structural design and thermal effects in order to maximize the photovoltaic efficiency.

Declaration of AI Assistance

The authors confirm that AI-based tools (ChatGPT, OpenAI) were used exclusively for language correction and editorial refinement to enhance clarity, grammar, and style. All scientific content, data analyses, and interpretations presented in the manuscript were conceived, developed, and rigorously verified solely by the authors.

References.

[1] X. Huang et al., "High-temperature polarization-free III-nitride solar cells with self-cooling effects," ACS Photonics, vol. 6, no. 8, pp. 2096-2103, 2019. https://doi.org/10.1021/acsphotonics.9b00655

[2] J. J. Williams et al., "Development of a high-band gap high temperature III-nitride solar cell for integration with concentrated solar power technology," in 2016 IEEE 43rd Photovoltaic Specialists Conference (PVSC), 2016: IEEE, pp. 0193-0195. https://doi.org/10.1109/PVSC.2016.7749576

[3] D. J. Sirbuly, M. Law, H. Yan, and P. Yang, "Semiconductor nanowires for subwavelength photonics integration," vol. 109, ed: ACS Publications, 2005, pp. 15190-15213. https://doi.org/10.1021/jp051813i

[4] F. Ponce and D. Bour, "Nitride-based semiconductors for blue and green light-emitting devices," nature, vol. 386, no. 6623, pp. 351-359, 1997. https://doi.org/10.1038/386351a0

[5] L. E. Bain and A. Ivanisevic, "Engineering the Cell-Semiconductor Interface: A Materials Modification Approach using II-VI and III-V Semiconductor Materials," Small, vol. 11, no. 7, pp. 768-780, 2015. https://doi.org/10.1002/smll.201401450

[6] S. Nakamura, T. Mukai, and M. Senoh, "Candela-class high-brightness InGaN/AlGaN double-heterostructure blue-light-emitting diodes," Applied Physics Letters, vol. 64, no. 13, pp. 1687-1689, 1994. https://doi.org/10.1063/1.111832

[7] U. K. Mishra, L. Shen, T. E. Kazior, and Y.-F. Wu, "GaN-based RF power devices and amplifiers," Proceedings of the IEEE, vol. 96, no. 2, pp. 287-305, 2008. https://doi.org/10.1109/JPROC.2007.911060

[8] L. Vilbois, A. Cheknane, A. Bensaoula, C. Boney, and T. Benouaz, "Simulation of a solar cell based on InGaN," Energy Procedia, vol. 18, pp. 795-806, 2012. https://doi.org/10.1016/j.egypro.2012.05.095

[9] R. Singh, D. Doppalapudi, T. Moustakas, and L. Romano, "Phase separation in InGaN thick films and formation of InGaN/GaN double heterostructures in the entire alloy composition," Applied Physics Letters, vol. 70, no. 9, pp. 1089-1091, 1997. https://doi.org/10.1063/1.118493

[10] S. Routray and T. Lenka, "InGaN-based solar cells: a wide solar spectrum harvesting technology for twenty-first century," CSI Transactions on ICT, vol. 6, no. 1, pp. 83-96, 2018. https://doi.org/10.1007/s40012-017-0181-9

[11] O. Jani, I. Ferguson, C. Honsberg, and S. Kurtz, "Design and characterization of GaN/ InGaN solar cells," Applied Physics Letters, vol. 91, no. 13, 2007. https://doi.org/10.1063/1.2793180

[12] C. J. Neufeld, N. G. Toledo, S. C. Cruz, M. Iza, S. P. DenBaars, and U. K. Mishra, "High quantum efficiency InGaN/GaN solar cells with 2.95 eV band gap," Applied Physics Letters, vol. 93, no. 14, 2008. https://doi.org/10.1063/1.2988894

[13] H. Abboudi et al., "Optimization of InxGa1− xN PIN Solar Cells: Achieving 21% Efficiency Through SCAPS-1D Modeling," Crystals, vol. 15, no. 7, p. 633, 2025. https://doi.org/10.3390/cryst15070633

[14] T. Ouslimane, L. Et-Taya, L. Elmaimouni, and A. Benami, "Impact of absorber layer thickness, defect density, and operating temperature on the performance of MAPbI3 solar cells based on ZnO electron transporting material," Heliyon, vol. 7, no. 3, 2021. https://doi.org/10.1016/j.heliyon.2021.e06379

[15] M. Minbashi, A. Ghobadi, M. H. Ehsani, H. Rezagholipour Dizaji, and N. Memarian, "Simulation of high efficiency SnS-based solar cells with SCAPS," Solar Energy, vol. 176, pp. 520-525, 2018/12/01/ 2018. https://doi.org/10.1016/j.solener.2018.10.058

[16] I. Vurgaftman and J. n. Meyer, "Band parameters for nitrogen-containing semiconductors," Journal of applied physics, vol. 94, no. 6, pp. 3675-3696, 2003. https://doi.org/10.1063/1.1600519

[17] Y. Varshni, "Band-to-Band Radiative Recombination in Groups IV, VI," February 1, vol. 19, p. 459, 2022. https://doi.org/10.1515/9783112498309-001

[18] Y. P. Varshni, "Temperature dependence of the energy gap in semiconductors," Physica, vol. 34, no. 1, pp. 149-154, 1967/01/01/ 1967. https://doi.org/10.1016/0031-8914(67)90062-6

[19] H. Abboudi et al., "Enhancing the Photovoltaic Efficiency of In0.2Ga0.8N/GaN Quantum Well Intermediate Band Solar Cells Using Combined Electric and Magnetic Fields," Materials, vol. 17, no. 21, p. 5219, 2024. [Online]. Available: https://www.mdpi.com/1996-1944/17/21/5219. https://doi.org/10.3390/ma17215219

[20] H. Abboudi et al., "Tuning Intermediate Band Solar Cell Efficiency: The Interplay of Electric Fields, Composition, Impurities, and Confinement," Nanomaterials, vol. 14, no. 22, p. 1858, 2024. [Online]. Available: https://www.mdpi.com/2079-4991/14/22/1858. https://doi.org/10.3390/nano14221858

[21] C. A. M. Fabien and W. A. Doolittle, "Guidelines and limitations for the design of high-efficiency InGaN single-junction solar cells," Solar Energy Materials and Solar Cells, vol. 130, pp. 354-363, 2014/11/01/ 2014. https://doi.org/10.1016/j.solmat.2014.07.018